

RESEARCH

Open Access



Gene co-expression network analysis of *Trypanosoma brucei* in tsetse fly vector

Kennedy W. Mwangi^{1,2*} , Rosaline W. Macharia³ and Joel L. Bargul^{1,2}

Abstract

Background: *Trypanosoma brucei* species are motile protozoan parasites that are cyclically transmitted by tsetse fly (genus *Glossina*) causing human sleeping sickness and nagana in livestock in sub-Saharan Africa. African trypanosomes display digenetic life cycle stages in the tsetse fly vector and in their mammalian host. Experimental work on insect-stage trypanosomes is challenging because of the difficulty in setting up successful *in vitro* cultures. Therefore, there is limited knowledge on the trypanosome biology during its development in the tsetse fly. Consequently, this limits the development of new strategies for blocking parasite transmission in the tsetse fly.

Methods: In this study, RNA-Seq data of insect-stage trypanosomes were used to construct a *T. brucei* gene co-expression network using the weighted gene co-expression analysis (WGCNA) method. The study identified significant enriched modules for genes that play key roles during the parasite's development in tsetse fly. Furthermore, potential 3' untranslated region (UTR) regulatory elements for genes that clustered in the same module were identified using the Finding Informative Regulatory Elements (FIRE) tool.

Results: A fraction of gene modules (12 out of 27 modules) in the constructed network were found to be enriched in functional roles associated with the cell division, protein biosynthesis, mitochondrion, and cell surface. Additionally, 12 hub genes encoding proteins such as RNA-binding protein 6 (RBP6), arginine kinase 1 (AK1), *brucei* alanine-rich protein (BARP), among others, were identified for the 12 significantly enriched gene modules. In addition, the potential regulatory elements located in the 3' untranslated regions of genes within the same module were predicted.

Conclusions: The constructed gene co-expression network provides a useful resource for network-based data mining to identify candidate genes for functional studies. This will enhance understanding of the molecular mechanisms that underlie important biological processes during parasite's development in tsetse fly. Ultimately, these findings will be key in the identification of potential molecular targets for disease control.

Keywords: *Trypanosoma brucei*, Tsetse fly, Gene co-expression network, Weighted gene co-expression network analysis

Background

Trypanosoma brucei has a digenetic life cycle with distinct morphological forms existing during its development in the mammalian host and the tsetse fly [1]. In the mammalian bloodstream, the morphological forms are

slender and stumpy trypomastigotes, while in the tsetse fly, they comprise procyclic trypomastigote forms in the midgut, long and short epimastigotes in the proventriculus, and short epimastigote and metacyclic trypomastigotes in the salivary glands [2, 3]. Most *T. brucei* research has focused on the mammalian bloodstream and tsetse procyclic forms of trypanosomes as they are relatively easier to maintain in *in vitro* cultures [4, 5]. Consequently, this has led to less exploration of parasite phenotypes in the tsetse fly that could provide insights into

*Correspondence: wanjaukm@gmail.com

² Jomo Kenyatta University of Agriculture and Technology, P.O. BOX 62000-00200, Nairobi, Kenya

Full list of author information is available at the end of the article



© The Author(s) 2021. This article is licensed under a Creative Commons Attribution 4.0 International License, which permits use, sharing, adaptation, distribution and reproduction in any medium or format, as long as you give appropriate credit to the original author(s) and the source, provide a link to the Creative Commons licence, and indicate if changes were made. The images or other third party material in this article are included in the article's Creative Commons licence, unless indicated otherwise in a credit line to the material. If material is not included in the article's Creative Commons licence and your intended use is not permitted by statutory regulation or exceeds the permitted use, you will need to obtain permission directly from the copyright holder. To view a copy of this licence, visit <http://creativecommons.org/licenses/by/4.0/>. The Creative Commons Public Domain Dedication waiver (<http://creativecommons.org/publicdomain/zero/1.0/>) applies to the data made available in this article, unless otherwise stated in a credit line to the data.

the biology of a trypanosome during its development in the vector—the life cycle phase referred to as “the heart of darkness” [6]. The knowledge of trypanosome development in the tsetse fly will contribute to efforts towards interrupting disease transmission by the vector. This can be achieved through targeted disruption of the parasite’s essential molecular processes such as motility, regulation of differentiation, morphological remodeling, and signal transduction [7, 8].

In the last decade, RNA-Seq technology has been a fundamental tool for studying gene expression profiles of *T. brucei* and other kinetoplastids with an aim of expanding knowledge on their biology [9]. This is because RNA-Seq provides a comprehensive and more accurate transcriptome quantification and characterization compared to the hybridization-based techniques such as microarray [10]. In addition to identification of differentially expressed genes, transcriptome data could also be used to create gene co-expression networks which provide a functional and molecular understanding of key biological processes in an organism [11, 12].

Gene co-expression network analysis aims to identify coordinated gene expression patterns that indicate functional relationships between the expressed genes. Using a method such as WGCNA [13], highly correlated genes are grouped into modules (gene clusters) which are currently thought to be co-expressed and hence perform similar biological functions [14]. Each module is believed to encode a specific biological function based on the genes it contains. To associate genes in a given module to specific functions, an enrichment analysis is performed against databases such as gene ontology (GO) [15] and Kyoto Encyclopedia for Genes and Genomes (KEGG) [16].

Furthermore, WGCNA allows identification of intra-modular hub genes, which are usually the highly connected genes in a module [13, 17]. These hub genes could play key roles in the biological functions of their modules or act as representatives of their predominant biological function [11]. Also, based on the hypothesis that functionally related genes may be co-regulated, co-expression network modules are useful in gene regulation analysis including prediction of regulatory elements (motifs) for genes in the same module [18, 19]. Additionally, functions of uncharacterized genes are predicted based on their co-expression with genes of known function in the co-expression network, a principle referred to as “guilt by association” [12].

The present study aimed at generating a gene co-expression network to explore functionally relevant genes involved in *T. brucei* development in the tsetse fly vector. In contrast to a *T. brucei* gene co-expression network generated from a previous study for procyclic and

bloodstream forms using microarray data [20], our study focused on the insect stage morphological forms of the parasite by analyzing RNA-Seq data. The constructed gene co-expression network permitted identification of 12 functionally relevant modules and their 12 hub genes as well as potential regulatory motifs in the mRNA’s 3’ untranslated regions for genes grouped in the same module.

Methods

Datasets acquisition and quality assessment

RNA-Seq datasets of *Glossina morsitans morsitans* (tsetse fly) trypanosome-infected midgut, proventriculus, and salivary gland tissues were obtained from the European Nucleotide Archive (ENA) [21] under accession numbers SRP002243 and SRR965341. The dataset consisted of 18 samples: 7 midgut; 4 proventriculus; 7 salivary glands [22, 23]. The quality of the data was assessed using FastQC version 0.11.8 (<http://www.bioinformatics.babraham.ac.uk/projects/fastqc/>). Prior to reads mapping, the *T. brucei* genome and *G. morsitans* scaffold genome were obtained from TriTrypDB (Release 43) [24] and VectorBase [25], respectively, and concatenated to create a chimeric genome. The RNA-Seq reads were mapped to the chimeric genome of *T. brucei* and *G. morsitans* using HISAT2 version 2.1.0 [26] to remove ambiguously mapped reads. Duplication rates were computed after read mapping using the MarkDuplicates tool from Picard toolkit version 2.20.3 (<http://broadinstitute.github.io/picard/>) to mark duplicate reads. Furthermore, dupRadar Bioconductor R package version 1.18.0 was used to assess the RNA-Seq data for presence of PCR duplicates [27]. Samples that had PCR duplicates were excluded from downstream analysis.

Reads quantification

The reads that mapped to *T. brucei* genome were counted using HTSeq version 0.11.2 [28] and in relation to the annotation file of *T. brucei* downloaded from TriTrypDB (Release 43). Non-protein coding genes (ncRNA, snRNA, snoRNA, pseudogenic transcripts, rRNA, and tRNA) were excluded from the read counts as this study focused on protein-coding genes and their functional analysis.

Sample quality assessment and filtering

Genes with low expression levels were removed from the read counts data using *filterByExpr* function from R package edgeR version 3.8 [29]. Sample quality was assessed using Pearson correlation heatmaps and Principal Component Analysis (PCA) and box plots in R version 3.6.0 [30]. Trimmed mean of M-values (TMM) was used as a normalization method using *calcNormFactors* function in edgeR [29]. The normalized read counts were

then converted to counts per million and \log_2 transformed for downstream analysis. Batch effects were adjusted for using the ComBat method from sva R package version 3.32.1 [31].

Construction of the weighted gene co-expression network

The weighted gene co-expression network was constructed using WGCNA R package version 1.66 [17]. First, soft-thresholding power, β , was determined using the *pickSoftThreshold* function from WGCNA package. This was followed by the construction of a weighted adjacency matrix using the *adjacency* function, after which the matrix was computed into the Topological Overlap Matrix (TOM) using the *TOMsimilarity* function [13]. The TOM measure between pairs of genes was used as input for average linkage hierarchical clustering by first creating a dissimilarity matrix ($\text{dissTOM} = 1 - \text{TOM}$) and then using the *flashClust* function to create the gene tree dendrogram. The Dynamic Tree Cut algorithm was used to identify modules using the gene tree dendrogram as input for the *cutreeDynamicTree* function from dynamicTreeCut R package version 1.63-1 [32]. The *chooseTopHubInEachModule* function from the WGCNA package was used to identify the hub genes.

Network functional enrichment analysis and visualization

The goseq R package version 1.36.0 [33] was used to test for enrichment of gene ontology (GO) [15] and Kyoto Encyclopedia of Gene and Genomes (KEGG) [16] annotations for each of the identified modules. The GO and KEGG annotations were obtained from TriTrypDB. The generated lists of GO terms for the modules were summarized using REVIGO (<http://revigo.irb.hr/>) [34]. Cytoscape version 3.7.1 [35] was used to visualize the network using the *exportNetworkToCytoscape* function from the WGCNA package.

Prediction of 3' UTR regulatory motifs

All the genes in the gene co-expression network and their corresponding cluster/module index were used to generate an expression file that was used as input for the tool FIRE, version 1.1a [19]. This expression file was submitted online to FIRE (<https://tavazoielab.c2b2.columbia.edu/FIRE/>) with default parameters for prediction of 3' UTR motifs.

The code used in data pre-processing, network construction, and functional analysis is provided as Additional file 1 and archived at: https://github.com/wanjauk/tbrucei_gcn. Motif prediction was performed online at: <https://tavazoielab.c2b2.columbia.edu/FIRE/>.

Results

Data pre-processing

A total of 18 samples of raw RNA-Seq data (Additional file 2: Table S1) were obtained for this study. Of the 18 samples, 3 generated from the trypanosome-infected salivary glands were excluded from further analysis because they contained PCR duplicates. Thus, a total of 15 samples were analyzed (Additional file 2: Table S1). Furthermore, lowly expressed genes were excluded to reduce noise, thus resulting in a total of 7390 genes across the 15 samples.

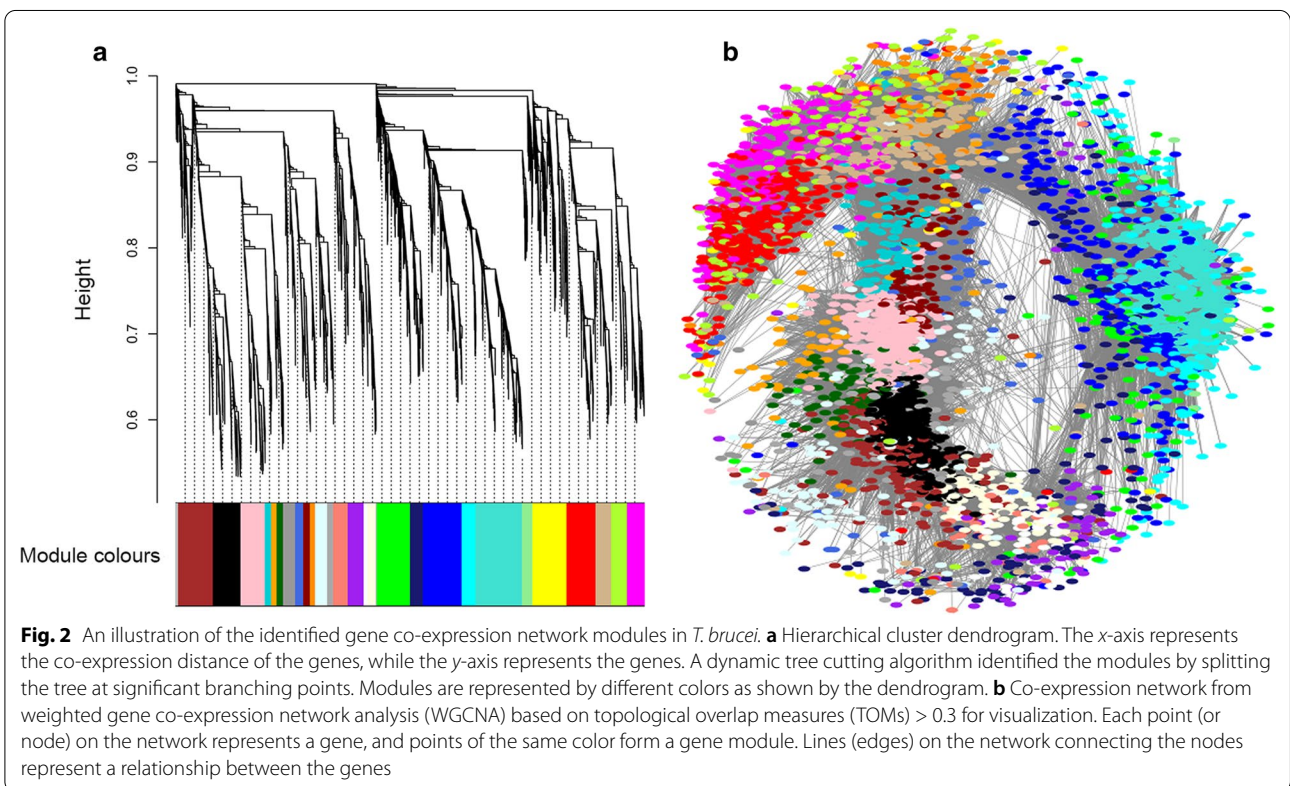
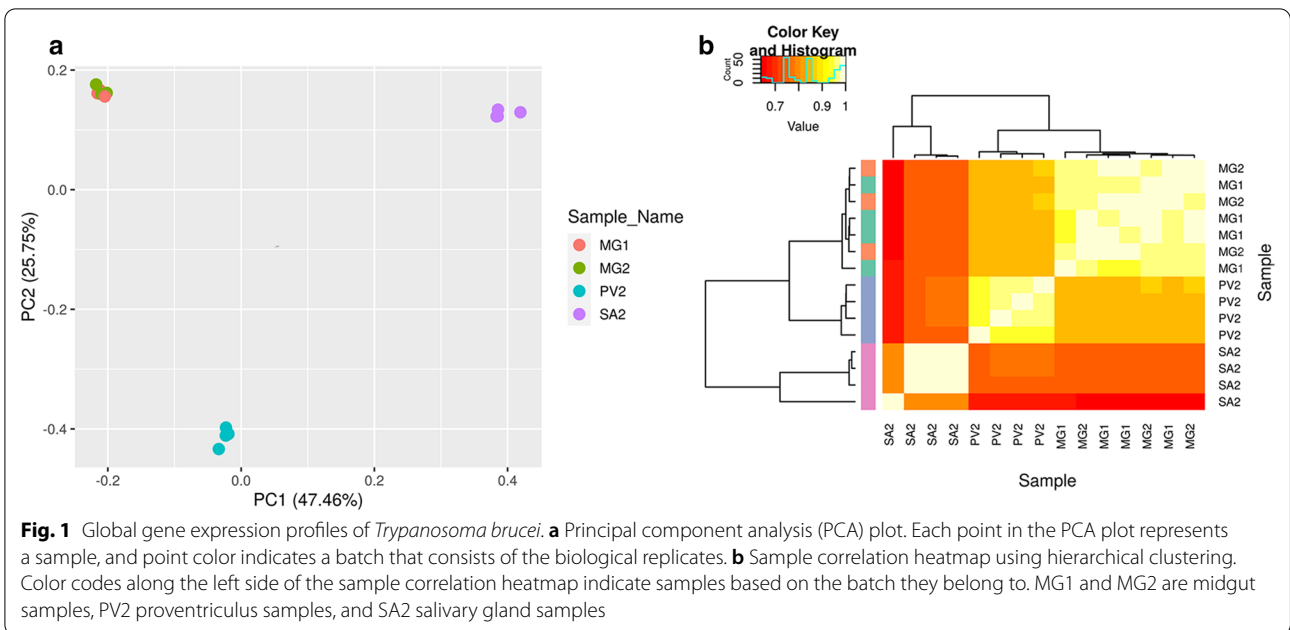
The relationship between the samples and the reproducibility of biological replicates was determined using principal component analysis (PCA) and Pearson correlation heatmap analysis prior to (Additional file 3: Figure S1) and after adjusting for batch effects that could have resulted from biological replicates (Fig. 1). The PCA and Pearson correlation heatmap plots showed that the samples grouped together based on the developmental stages of *T. brucei* in the insect vector rather than their biological replicates (Fig. 1). An assessment of the distribution of per-gene read counts per sample showed a median steady-state expression level of $\sim 6.5 \log_2$ counts per million in all the 15 samples (Additional file 4: Figure S2).

Weighted gene co-expression network construction

A total of 7390 protein coding genes from 15 samples were used for the construction of the co-expression network. Prior to generation of the network, the soft-thresholding power to which co-expression similarity was raised to calculate adjacency was determined by analysis of thresholding powers from 1 to 20. Power 14, the power for which the scale-free topology fitting index (R^2) was ≥ 0.8 , was chosen (Additional file 5: Figure S3). A total of 28 distinct modules were generated for 7390 protein coding genes from the hierarchical clustering tree (dendrogram) using the dynamic tree cut algorithm (Figs. 2, 3, and Additional file 6: Table S2). The gray module, which contained 59 genes that could not be assigned to any module, was excluded from the analysis (Fig. 3). Thus, a total of 27 modules were used in the subsequent analysis. The module with the least genes (61) was the white module while the turquoise module had the largest number of genes (732) (Fig. 3).

Functional and pathway enrichment analysis

Out of the 27 modules generated, only 14 modules were found to be enriched for GO terms; 12 were over-represented and 2 (blue and green modules) were under-represented for GO terms (Additional file 7: Table S3). Seven of the 27 modules were enriched following KEGG pathway enrichment analysis, from which 5 were



over-represented and 2 (lightcyan and blue modules) were under-represented for KEGG pathway terms (Additional file 8: Table S4). The top enriched GO terms for the modules with over-represented GO terms highlight some

functions of the module genes (Table 1). Of the 12 modules with over-represented GO terms, 4 modules were over-represented for KEGG pathway terms and 1 module

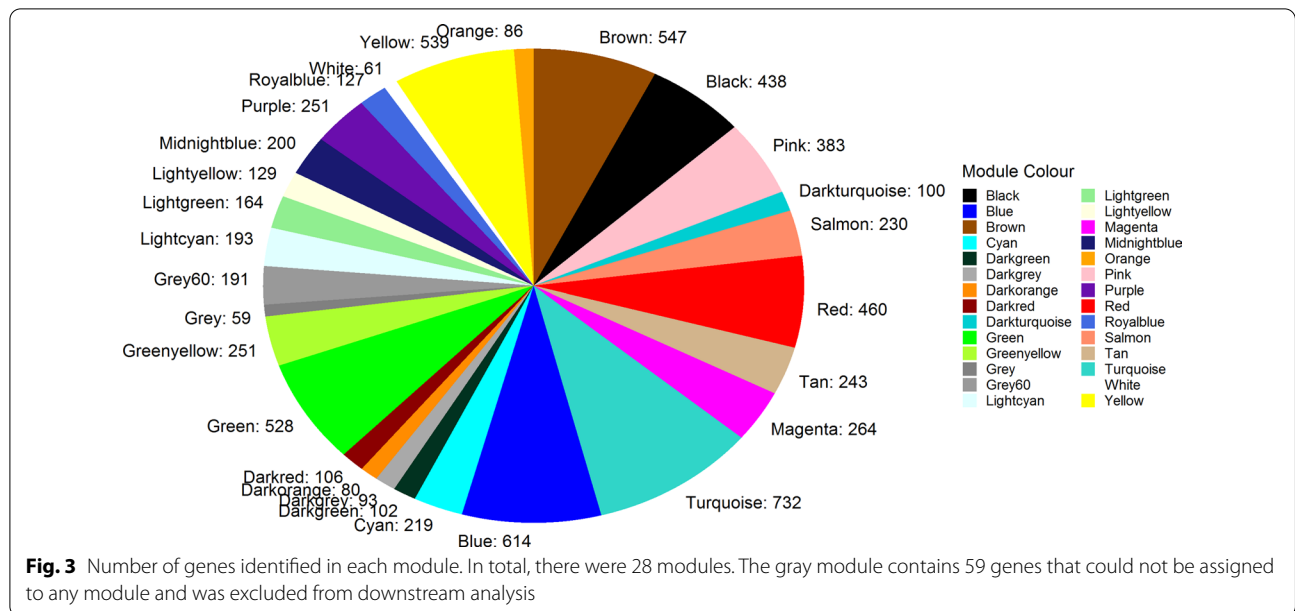


Table 1 Modules with over-represented GO terms and their most significant over-represented GO and KEGG pathway terms

Module	Top enriched GO term	GO term adjusted <i>p</i> value	KEGG pathways term	KEGG term adjusted <i>p</i> -value
Brown	Adenylate cyclase activity	1.151E-02	–	–
Black	Cellular nitrogen compound biosynthetic process	2.779E-07	–	–
Pink	Cytochrome complex	4.917E-02	RNA transport	3.187E-02
Darkturquoise	Transferase activity, transferring phosphorus-containing groups	1.815E-02	–	–
Salmon	RNA binding	2.191E-03	–	–
Purple	Mitochondrial protein complex	1.093E-06	–	–
Lightyellow	Structural constituent of ribosome	6.262E-11	Ribosome	9.416E-08
Turquoise	Cell surface	2.395E-04	–	–
Red	Cytoskeletal part	7.976E-04	Homologous recombination	1.478E-02
Tan	Spindle pole	4.930E-02	–	–
Greenyellow	Cytoskeleton	1.211E-03	–	–
Magenta	Cytoskeleton	3.979E-04	Purine metabolism	9.042E-03
Yellow	–	–	Endocytosis	2.502E-02

“–” indicates detection of no significant GO or KEGG terms

(yellow module) was over-represented for a KEGG pathway term (endocytosis), but not GO terms (Table 1).

Modules hub gene identification

Highly connected genes in a module are referred to as intra-modular hub genes. These hub genes are considered functionally significant in the enriched functions of the modules. Following the hypothesis that higher connectivity for a gene implies more importance in the module’s functional role, genes with the highest connectivity in the 27 modules were determined and considered to

be the hub genes (Additional file 9: Table S5). Hub genes for the 12 modules with over-represented GO terms are described in Table 2.

3’ UTR motif prediction based on gene co-expression modules

Genes in a given module are hypothesized to be co-regulated as they are assumed to have similar functions. Consequently, their *cis*-regulatory element should be similar. Following this hypothesis, ten statistically

Table 2 Identified hub genes and their encoding proteins for the 12 modules with over-represented GO terms

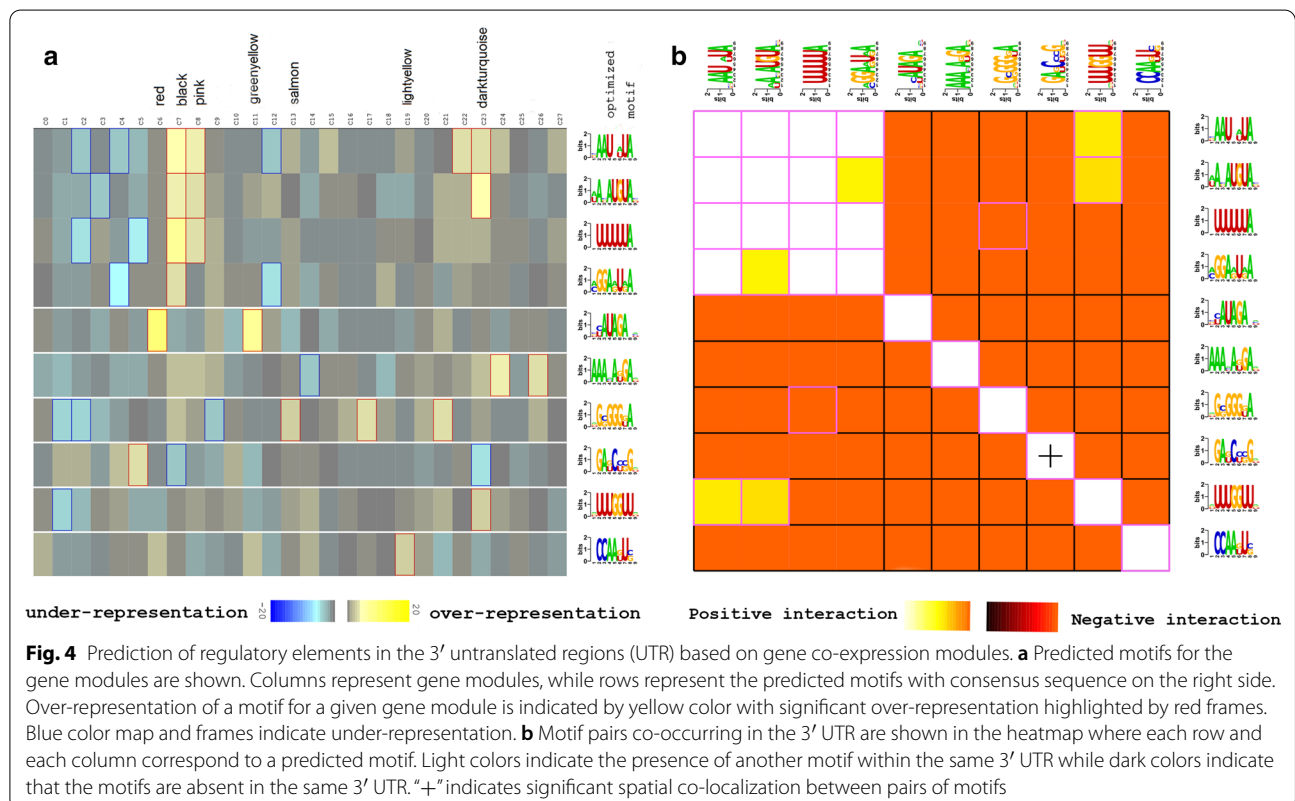
Module	Hub gene	Encoding protein
Brown	Tb927.11.1570	Hypothetical protein, conserved
Black	Tb927.7.1790	Adenine phosphoribosyltransferase, putative
Pink	Tb927.10.6200	Hypothetical protein, conserved
Darkturquoise	Tb927.8.6650	RNA-binding protein, putative
Salmon	Tb927.11.1450	2-Oxoglutarate dehydrogenase E1 component, putative
Purple	Tb927.1.600	Phosphate-repressible phosphate permease, putative
Lightyellow	Tb927.10.2560	Mitochondrial malate dehydrogenase
Red	Tb927.7.6920	Hypothetical protein, conserved
Tan	Tb927.3.2930	RNA-binding protein RBP6, putative
Greenyellow	Tb927.7.920	Inner arm dynein 5-1
Magenta	Tb927.9.6290	Arginine kinase
Turquoise	Tb927.9.15630	BARP protein

significant RNA motifs, each over-represented in different gene modules, were identified using FIRE (Fig. 4a).

Discussion

This study employed the WGCNA method [17] to construct the *T. brucei* weighted gene co-expression network using RNA-Seq data. The resulting co-expression network analysis allowed identification of modules (gene

clusters) as well as enrichment analysis in GO [15] and KEGG [16] annotation databases to associate the modules with their functions. Highly connected genes in a module, known as intra-modular hub genes [17], were also determined as they are key drivers of a molecular process or act as a representative of the predominant biological function of the module. Here, we demonstrate the usefulness of the network for functional genomic analysis



using an example of the cell cycle and protein biosynthesis enriched functions.

The cell cycle in eukaryotes comprises four phases, namely: G_0/G_1 , S, G_2 , and M phases [36]. The cell prepares for division in the first gap phase (G_0/G_1), replicates the DNA during the S phase, and then undergoes mitosis (M) in the second gap phase (G_2). In *T. brucei*, the cell cycle is tightly regulated to ensure that single-copy organelles and structures such as the Golgi body, mitochondrion, kinetoplast, nucleus, basal body, and flagellum are duplicated, maintained at precise positions in the cell and segregated accurately [37]. Various GO terms related to organelles were over-represented in the black module (Figs. 2 and 3) and included microbody, peroxisome, glycosome, and acidocalcisome (Additional file 10: Figure S4). The organelles duplicate in the first gap phase (G_0/G_1) [38]. This suggests that genes assigned to the black module (Figs. 2 and 3) could play a role in the cell cycle particularly during the G_0/G_1 phase. Furthermore, some cyclins and cdc2-related kinases (CRKs) that are key regulators of the cell cycle such as CYC2 (Tb927.11.14080), CYC5 (Tb927.10.11440), and CRK10 (Tb927.3.4670) were assigned to the black module (Additional file 6: Table S2). Both CY2 and CY5 regulate the transition of G_1 phase to S phase [39]. Co-expression of CRK10, whose regulatory role is presently unknown, with CYC2 and CYC5 and its demonstrated interaction with CYC2 in yeast two-hybrid assay [39] suggests a possible role in G_1 to S phase transition.

The hub gene for the black module was identified as adenine phosphoribosyltransferase (APRT) (Table 2), which plays a crucial role in the purine salvage pathway in *T. brucei*. This parasite lacks a de novo purine biosynthetic pathway [40]. Purine nucleotides are precursors of DNA and RNA and are also constituents of second messengers in signaling pathways such as cyclic AMP [41]. In this regard, APRT may be important in enriched module functions such as cyclic nucleotide biosynthesis and synthesis of the structural constituent of the ribosome, particularly ribosomal RNA, and consequently, signaling and protein biosynthesis. Signaling is depicted by the black module's over-represented GO terms such as adenylate cyclase activity, while protein biosynthesis is depicted by GO terms such as translation, unfolded protein binding, protein folding, and structural constituent of ribosome (Additional file 10: Figure S4).

The red module (Figs. 2 and 3) was functionally enriched for GO terms such as DNA replication and chromosome organization and the KEGG pathway term homologous recombination, indicating that its genes are involved in the progression of the cell cycle (Additional file 11: Figure S5 and Table 1). Additionally, the red module has some genes involved in cytokinesis such as

BOH1 (Tb927.10.12720), which cooperates with *TbPLK* to initiate cytokinesis and flagellum inheritance [42], and cytokinesis initiation factor 2 (CIF2) (Tb927.9.14290), which is involved in initiation of cytokinesis [43] (Additional file 6: Table S2). Other genes assigned to this module were in concordance with the enriched functions. These were nucleus- and spindle-associated protein 1 (NuSAP1) (Tb927.11.8370), which is required in chromosome segregation and NuSAP2 (Tb927.9.6110), which promotes the G_2/M transition [44]. The hub gene for the red module is a hypothetical gene (Tb927.7.6920), which may play a key role in the progression of the cell cycle.

The tan module (Figs. 2 and 3), whose enriched GO terms include the spindle pole and microtubule cytoskeleton, has genes such as CIF4 (Tb927.10.8240), TLK1 (Tb927.4.5180), and FPRC (Tb927.10.6360), which are involved in cytokinesis [45, 46]. The hub gene for the tan module is RNA-binding protein RBP6 (Table 2). Interestingly, over-expression of RBP6 *in vitro* has been demonstrated to recapitulate the parasite's tsetse fly stage developmental form, which was previously elusive in culture [47]. However, the exact role of RBP6 during the parasite's development in the tsetse fly is yet to be elucidated. Based on its assignment to the tan module, it is likely to be involved in regulating a key step during progression of the cell cycle.

The salmon module (Figs. 2 and 3) has enriched functions in RNA metabolic processing depicted by the module's enriched GO terms, which are RNA metabolism, nucleic acid binding, and RNA binding (Additional file 12: Figure S6). RNA binding may either involve binding of the mRNA by RNA-binding proteins (RBPs) as a post-transcriptional gene regulation mechanism in *T. brucei* [48, 49] or binding by translation initiation factors for protein synthesis [50]. The salmon module has translation initiation factor eIF4E1 (Tb927.11.2260) and poly(A) binding protein PABP2 (Tb927.9.10770), which have previously been shown to be co-localized in *T. brucei* [51]. An RNA-binding protein related to the stress response, ZC3H30 (Tb927.10.1540), together with an associated stress response granule (Tb927.8.3820) [52], was assigned to the salmon module. The hub gene for the salmon module is the 2-oxoglutarate dehydrogenase E1 component (Table 2). 2-Oxoglutarate dehydrogenase is an enzyme involved in the tricarboxylic acid (TCA) cycle in the mitochondrion implicated in the degradation of proline and glutamate to succinate, which can enter the gluconeogenesis pathway in procyclic trypanosomes [53]. This hub gene could be important in the role of the mitochondrion in responding to stress as a result of change in energy source in insect-stage trypanosomes.

Some genes that were identified as hub genes had previously been characterized through functional

studies. These include: inner arm dynein 5-1 (IAD5-1) (Tb927.7.920), which was identified as a hub gene for the greenyellow module. Knockdown of IAD5-1 through RNAi was shown to cause a defect in cell motility, indicating its functional role in the parasite's motility [54]. Yet another inner arm dynein gene, DNAH10 (Tb927.4.870), has been implicated in cell motility through RNAi knockdown functional studies [55]. In our study, both DNAH10 and IAD5-1 clustered in the greenyellow module which was highly enriched for GO terms associated with cytoskeleton and motility (Additional file 13: Figure S7), confirming previous functional roles in cell motility by [54, 55].

Additionally, RNAi knockdown of DRBD13 (Tb927.8.6650) has previously been found to be deleterious to parasite's growth in the tsetse fly by causing up-regulation of RBP6 (Tb927.3.2930) gene [56]. Both DRBD13 and RBP6 were identified as hub genes in the constructed network: DRBD13 was found in the darkturquoise module enriched for transfer of phosphorus-containing groups and RBP6 in the tan module enriched for cell cycle terms such as spindle pole. The RBP6 has been implicated in parasite development in the tsetse fly [47]. Its identification as a hub gene and congruence in its predicted function through this study confirms the usefulness of such *in silico* studies in selecting candidates for *in vitro* studies.

Regulation of gene expression in *T. brucei* occurs almost exclusively post-transcriptionally as a result of polycistronic arrangement of their genes [50, 57, 58]. Post-transcriptional regulation of mRNA abundance mainly involves interaction of their *cis*-regulatory element and a *trans*-acting element such as an RNA-binding protein [59]. Genes with similar functions are co-regulated together; thus, their mRNAs are hypothesized to have similar *cis*-regulatory elements [19]. Since the gene modules of a co-expression network are composed of genes with similar functions, they can be used as a basis for identifying potential regulatory elements in the untranslated regions of mRNA.

Two motifs ([AU]A[CGU]AUGUA[CGU] and [CGU][CU]AUAGA.[ACU]) that had consensus sequences similar to previously identified motifs were found to be over-represented (Fig. 4a). The motif [AU]A[CGU]AUGUA[CGU] contains the core sequence, UGUA, that is recognized by the PUF family of RNA-binding proteins [60] and has previously been identified in *T. brucei* as targeting transcripts involved in the cell cycle [61–63]. The motif was over-represented in the black, pink, and darkturquoise modules (Fig. 4a). [AU]A[CGU]AUGUA[CGU] co-occurs with other motifs including [CGU]AAU.[AU]UA., UUUUUUA., [AC]GGA[AG]U[AG]A. and [AGU]UUUGGUU[AGU]

(lighter colors in Fig. 4b). Co-occurrence of motifs means that they co-localize within the same untranslated region (UTR), which indicates that the presence of one motif implies the presence of its putative counterpart [19]. These co-occurring motifs may provide further information on post-transcriptional regulation. For instance, co-localization of two motifs close to each other on a transcript could imply physical interaction of their binding elements, hence their functional interaction [19].

The other motif, [CGU][CU]AUAGA.[ACU], was over-represented in the red and greenyellow modules (Fig. 4a). This consensus motif contains the core AUAGA sequence similar to CAUAGAA that has been implicated in cell cycle regulation [64, 65] and was previously predicted in *T. brucei* [63]. Notably, genes in the red module were enriched for cell cycle functions while those in the greenyellow module were enriched for microtubule-associated functions, including motility (Additional file 13: Figure S7). Motility in *T. brucei* is mediated through the flagellum [66]. Importantly, flagellum motility is essential for completion of the cell division [67, 68] suggesting co-regulation of genes in the greenyellow module together with those in the red module. The motif [CGU][CU]AUAGA.[ACU] does not co-occur with other motifs, which possibly suggests that its functions have opposing effects compared with functions of the other motifs (Fig. 4b). Overall, characterization of these identified *cis*-regulatory elements will advance our knowledge on post-transcription gene regulation and provide potential chemotherapeutic targets against key regulatory functions in *T. brucei* for disease control.

Conclusions

Construction of the *T. brucei* gene co-expression network provides a valuable resource for identifying candidate genes for experimental work. These candidate genes could be important in elucidating molecular mechanisms that underlie important biological processes during the parasite's development in tsetse fly. Our results indicate correspondence between the enriched functions of module genes, particularly the identified hub genes, and known *T. brucei* biology. This illustrates the effectiveness of the co-expression network analysis as an approach to explore functionally relevant genes in *T. brucei* development in tsetse fly. Furthermore, the hub genes from this study that encode proteins whose functional roles are still unknown could be used to inform research focus and priorities while performing *in vitro* studies. Knowledge on *T. brucei* development in the tsetse fly vector is crucial in identifying key targets to block transmission of these medically and economically important parasites.

Supplementary information

The online version contains supplementary material available at <https://doi.org/10.1186/s13071-021-04597-6>.

Additional file 1: Code used in data pre-processing, network construction, and functional analysis. It is archived at https://github.com/wanjauk/tbrucei_gcn.

Additional file 2: Table S1. Sample metadata for samples used in this study. Samples highlighted in red were excluded from analysis because of failing quality assessment

Additional file 3: Figure S1. Principal component analysis (PCA) and Pearson correlation heatmap prior to accounting for batch effects. **(a)** Each point in the PCA plot represents an experimental sample, and point color indicates a batch that consists of the biological replicates. **(b)** Color codes along the left side of the sample correlation heatmap indicate samples based on the batch they belong to. MG1 and MG2 are midgut samples, PV2 are proventriculus samples, and SA2 are salivary gland samples

Additional file 4: Figure S2. Assessment of per-gene read count distribution per sample using a boxplot. The distribution of per-gene read counts per sample showed a median steady-state expression level of $\sim 6.5 \log_2$ counts per million for all the 15 samples

Additional file 5: Figure S3. Scale-free topology plot for selecting the power β for the signed correlation network. **(a)** Scale free topology index (y axis) as a function of powers, β , 1 to 20 (x axis). **(b)** Mean connectivity (y axis) as a decreasing function of powers β (x axis)

Additional file 6: Table S2. Co-expression network genes comprising the modules of the network. There are a total of 7390 genes distributed across 28 modules in the co-expression network

Additional file 7: Table S3. Module GO enrichment results; 14 modules with their significantly over- and under-represented GO terms are tabulated

Additional file 8: Table S4. Module KEGG enrichment results; 7 modules with their significantly over- and under-represented KEGG terms are tabulated

Additional file 9: Table S5. Hub genes for all the 27 modules and the proteins they encode

Additional file 10: Figure S4. Black module over-represented GO terms. **(a)** Biological process GO terms; **(b)** cellular component GO terms; **(c)** molecular function GO terms

Additional file 11: Figure S5. Red module over-represented GO terms. **(a)** Biological process GO terms; **(b)** cellular component GO terms

Additional file 12: Figure S6. Salmon module over-represented GO terms. **(a)** Biological process GO terms; **(b)** molecular function GO terms

Additional file 13: Figure S7. Greenyellow module over-represented GO terms. **(a)** Biological process GO terms; **(b)** cellular component GO terms; **(c)** molecular function GO terms

Abbreviations

AK1: Arginine kinase 1; APRT: Adenine phosphoribosyltransferase; BARP: Brucei alanine-rich protein; BOH1: Bait on hook 1; CIF: Cytokinesis initiation factor; CRK: cdc2-related kinase; ENA: European Nucleotide Archive; FIRE: Finding informative regulatory elements; GO: Gene Ontology; KEGG: Kyoto Encyclopedia of Genes and Genomes; PABP: Poly(A) binding protein; PCA: Principal component analysis; RBP6: RNA-binding protein 6; TMM: Trimmed mean of M-values; TOM: Topological overlap matrix; UTR: Untranslated region; WGCNA: Weighted gene correlation network analysis.

Acknowledgements

We thank Dr. Caleb Kibet for his technical assistance during the study and Dr. Daniel Masiga and Dr. Jandouwe Villinger for insightful comments during the course of the study. The authors gratefully acknowledge the financial support for this research by the following organizations and agencies: UK's Foreign, Commonwealth & Development Office (FCDO); the Swedish International

Development Cooperation Agency (Sida); the Swiss Agency for Development and Cooperation (SDC); the Federal Democratic Republic of Ethiopia; and the Government of the Republic of Kenya. The views expressed herein do not necessarily reflect the official opinion of the donors.

Authors' contributions

KWM, RWM, JLB conceived and designed experiments. KWM performed experiments. RWM, JLB contributed reagents/materials/analysis tools. KWM, RWM, JLB analyzed data. KWM wrote the first manuscript draft. All authors read and approved the final manuscript.

Funding

This work was supported through the DELTAS Africa Initiative grant no. DEL-15-011 to THRIVE-2. The DELTAS Africa Initiative is an independent funding scheme of the African Academy of Sciences (AAS)'s Alliance for Accelerating Excellence in Science in Africa (AESA) and supported by the New Partnership for Africa's Development Planning and Coordinating Agency (NEPAD Agency) with funding from the Wellcome Trust, grant no. 107742/Z/15/Z, and the UK government. The views expressed in this publication are those of the author(s) and not necessarily those of AAS, NEPAD Agency, Wellcome Trust, or the UK government.

Availability of data and materials

The datasets supporting the conclusions of this study are included within the article and in the additional data files.

Ethics approval and consent to participate

Not applicable.

Consent for publication

Not applicable.

Competing interests

The authors declare that they have no competing interests.

Author details

¹ International Centre of Insect Physiology and Ecology (icipe), P.O. Box 30772-00100, Nairobi, Kenya. ² Jomo Kenyatta University of Agriculture and Technology, P.O. BOX 62000-00200, Nairobi, Kenya. ³ University of Nairobi, P.O. Box 30197-00100, Nairobi, Kenya.

Received: 16 September 2020 Accepted: 13 January 2021

Published online: 22 January 2021

References

- Vickerman K. Developmental cycles and biology of pathogenic trypanosomes. *Br Med Bull.* 1985;41:105–14.
- Sharma R, Peacock L, Gluenz E, Gull K, Gibson W, Carrington M. Asymmetric cell division as a route to reduction in cell length and change in cell morphology in trypanosomes. *Protist.* 2008;159:137–51.
- Dyer NA, Rose C, Ejeh NO, Acosta-Serrano A. Flying tsetse: survival and maturation of trypanosomes in tsetse flies. *Trends Parasitol.* 2013;29:188–96.
- Brun R, Schönenberger M. Cultivation and in vitro cloning or procyclic culture forms of *Trypanosoma brucei* in a semi-defined medium. Short communication. *Acta Trop.* 1979;36:289–92.
- Hirumi H, Doyle JJ, Hirumi K. Cultivation of bloodstream *Trypanosoma brucei*. *Bull World Health Organ.* 1977;55:405–9.
- Sharma R, Gluenz E, Peacock L, Gibson W, Gull K, Carrington M. The heart of darkness: growth and form of *Trypanosoma brucei* in the tsetse fly. *Trends Parasitol.* 2009;25:517–24.
- Ooi C-P, Bastin P. More than meets the eye: understanding *Trypanosoma brucei* morphology in the tsetse. *Front Cell Infect Microbiol.* 2013;3:71.
- Abbeele JVD, Rotureau B. New insights in the interactions between African trypanosomes and tsetse flies. *Front Cell Infect Microbiol.* 2013;3:63.
- Patino LH, Ramirez JD. RNA-seq in kinetoplastids: A powerful tool for the understanding of the biology and host-pathogen interactions. *Infect Genet Evol J Mol Epidemiol Evol Genet Infect Dis.* 2017;49:273–82.

10. Marioni JC, Mason CE, Mane SM, Stephens M, Gilad Y. RNA-seq: an assessment of technical reproducibility and comparison with gene expression arrays. *Genome Res.* 2008;18:1509–17.
11. Barabási A-L, Oltvai ZN. Network biology: understanding the cell's functional organization. *Nat Rev Genet.* 2004;5:101–13.
12. Wolfe CJ, Kohane IS, Butte AJ. Systematic survey reveals general applicability of “guilt-by-association” within gene coexpression networks. *BMC Bioinform.* 2005;6:227.
13. Zhang B, Horvath S. A general framework for weighted gene co-expression network analysis. *Stat Appl Genet Mol Biol.* 2005;4:Article 17.
14. van Dam S, Vösa U, van der Graaf A, Franke L, de Magalhães JP. Gene co-expression analysis for functional classification and gene–disease predictions. *Brief Bioinform.* 2018;19:575–92.
15. Ashburner M, Ball CA, Blake JA, Botstein D, Butler H, Cherry JM, et al. Gene Ontology: tool for the unification of biology. *Nat Genet.* 2000;25:25–9.
16. Kanehisa M, Goto S. KEGG: Kyoto Encyclopedia of Genes and Genomes. *Nucleic Acids Res.* 2000;28:27–30.
17. Langfelder P, Horvath S. WGCNA: an R package for weighted correlation network analysis. *BMC Bioinform.* 2008;9:559.
18. van Helden J, André B, Collado-Vides J. Extracting regulatory sites from the upstream region of yeast genes by computational analysis of oligonucleotide frequencies. *J Mol Biol.* 1998;281:827–42.
19. Elemento O, Slonim N, Tavazoie S. A universal framework for regulatory element discovery across all genomes and data-types. *Mol Cell.* 2007;28:337–50.
20. Shateri Najafabadi H, Salavati R. Functional genome annotation by combined analysis across microarray studies of *Trypanosoma brucei*. *PLoS Negl Trop Dis.* 2010;4:e810.
21. Leinonen R, Akhtar R, Birney E, Bower L, Cerdeno-Tárraga A, Cheng Y, et al. The European Nucleotide Archive. *Nucleic Acids Res.* 2011;39:D28–31.
22. Telleria EL, Benoit JB, Zhao X, Savage AF, Regmi S, Silva TLA, et al. Insights into the trypanosome-host interactions revealed through transcriptomic analysis of parasitized Tsetse fly salivary glands. *PLoS Negl Trop Dis.* 2014;8:e2649.
23. Savage AF, Kolev NG, Franklin JB, Vigneron A, Aksoy S, Tschudi C. Transcriptome profiling of *Trypanosoma brucei* development in the tsetse fly vector *Glossina morsitans*. *PLoS ONE.* 2016;11:e0168877.
24. Aslett M, Aurrecochea C, Berriman M, Brestelli J, Brunk BP, Carrington M, et al. TriTrypDB: a functional genomic resource for the Trypanosomatidae. *Nucleic Acids Res.* 2010;38:D457–62.
25. Lawson D, Arensburg P, Atkinson P, Besansky NJ, Bruggner RV, Butler R, et al. VectorBase: a home for invertebrate vectors of human pathogens. *Nucleic Acids Res.* 2007;35:D503–5.
26. Kim D, Langmead B, Salzberg SL. HISAT: a fast spliced aligner with low memory requirements. *Nat Methods.* 2015;12:357–60.
27. Sayols S, Scherzinger D, Klein H. dupRadar: a Bioconductor package for the assessment of PCR artifacts in RNA-Seq data. *BMC Bioinform.* 2016;17:428.
28. Anders S, Pyl PT, Huber W. HTSeq—a Python framework to work with high-throughput sequencing data. *Bioinformatics.* 2015;31:166–9.
29. Robinson MD, McCarthy DJ, Smyth GK. edgeR: a Bioconductor package for differential expression analysis of digital gene expression data. *Bioinformatics.* 2010;26:139–40.
30. R Core Team. R: A Language and Environment for Statistical Computing [Internet]. Vienna, Austria: R Foundation for Statistical Computing; 2019. <https://www.r-project.org/>.
31. Leek JT, Johnson WE, Parker HS, Jaffe AE, Storey JD. The sva package for removing batch effects and other unwanted variation in high-throughput experiments. *Bioinformatics.* 2012;28:882–3.
32. Langfelder P, Zhang B, Horvath S. Defining clusters from a hierarchical cluster tree: the Dynamic Tree Cut package for R. *Bioinformatics.* 2008;24:719–20.
33. Young MD, Wakefield MJ, Smyth GK, Oshlack A. Gene ontology analysis for RNA-seq: accounting for selection bias. *Genome Biol.* 2010;11:R14.
34. Supek F, Bošnjak M, Škunca N, Šmuc T. REVIGO summarizes and visualizes long lists of gene ontology terms. *PLoS ONE.* 2011;6:e21800.
35. Shannon P, Markiel A, Ozier O, Baliga NS, Wang JT, Ramage D, et al. Cytoscape: a software environment for integrated models of biomolecular interaction networks. *Genome Res.* 2003;13:2498–504.
36. Hammarton TC. Cell cycle regulation in *Trypanosoma brucei*. *Mol Biochem Parasitol.* 2007;153:1–8.
37. Wheeler RJ, Gull K, Sunter JD. Coordination of the cell cycle in trypanosomes. *Annu Rev Microbiol.* 2019;73:133–54.
38. Zhou Q, Hu H, Li Z. New Insights into the Molecular Mechanisms of Mitosis and Cytokinesis in Trypanosomes. *Int Rev Cell Mol Biol.* 2014;308:127–66.
39. Liu Y, Hu H, Li Z. The cooperative roles of PHO80-like cyclins in regulating the G1/S transition and posterior cytoskeletal morphogenesis in *Trypanosoma brucei*. *Mol Microbiol.* 2013;90:130–46.
40. Hammond DJ, Gutteridge WE. Purine and pyrimidine metabolism in the Trypanosomatidae. *Mol Biochem Parasitol.* 1984;13:243–61.
41. Ślepokura KA. Purine 3':5'-cyclic nucleotides with the nucleobase in a *syn* orientation: cAMP, cGMP and cIMP. *Acta Crystallogr Sect C Struct Chem.* 2016;72:465–79.
42. Pham KTM, Zhou Q, Kurasawa Y, Li Z. BOH1 cooperates with Polo-like kinase to regulate flagellum inheritance and cytokinesis initiation in *Trypanosoma brucei*. *J Cell Sci.* 2019;132:jcs230581.
43. Zhou Q, Hu H, Li Z. An EF-hand-containing protein in *Trypanosoma brucei* regulates cytokinesis initiation by maintaining the stability of the cytokinesis initiation factor CIF1. *J Biol Chem.* 2016;291:14395–409.
44. Zhou Q, Lee KJ, Kurasawa Y, Hu H, An T, Li Z. Faithful chromosome segregation in *Trypanosoma brucei* requires a cohort of divergent spindle-associated proteins with distinct functions. *Nucleic Acids Res.* 2018;46:8216–31.
45. Li Z, Umeyama T, Wang CC. The chromosomal passenger complex and a mitotic kinesin interact with the tousel-like kinase in trypanosomes to regulate mitosis and cytokinesis. *PLoS ONE.* 2008;3:e3814.
46. Hu H, An T, Kurasawa Y, Zhou Q, Li Z. The trypanosome-specific proteins FPRC and CIF4 regulate cytokinesis initiation by recruiting CIF1 to the cytokinesis initiation site. *J Biol Chem.* 2019;294:16672–83.
47. Kolev NG, Ramey-Butler K, Cross GAM, Ullu E, Tschudi C. Developmental progression to infectivity in *Trypanosoma brucei* Triggered by an RNA-binding protein. *Science.* 2012;338:1352–3.
48. Clayton C. The regulation of trypanosome gene expression by RNA-binding proteins. *PLoS Pathog.* 2013;9:e1003680.
49. Kolev NG, Ullu E, Tschudi C. The emerging role of RNA-binding proteins in the life cycle of *Trypanosoma brucei*. *Cell Microbiol.* 2014;16:482–9.
50. Clayton C, Shapira M. Post-transcriptional regulation of gene expression in trypanosomes and leishmanias. *Mol Biochem Parasitol.* 2007;156:93–101.
51. Kramer S, Bannerman-Chukualim B, Ellis L, Boulden EA, Kelly S, Field MC, et al. Differential localization of the two *T. brucei* Poly(A) binding proteins to the nucleus and RNP granules suggests binding to distinct mRNA pools. *PLoS ONE.* 2013;8:e54004.
52. Chakraborty C, Clayton C. Stress susceptibility in *Trypanosoma brucei* lacking the RNA-binding protein ZC3H30. *PLoS Negl Trop Dis.* 2018;12:e0006835.
53. van Weelden SWH, van Hellemond JJ, Opperdoes FR, Tielens AGM. New functions for parts of the Krebs cycle in procyclic *Trypanosoma brucei*, a cycle not operating as a cycle. *J Biol Chem.* 2005;280:12451–60.
54. Wei Y, Hu H, Lun Z-R, Li Z. Centrin3 in trypanosomes maintains the stability of a flagellar inner-arm dynein for cell motility. *Nat Commun.* 2014;5:4060.
55. Zukas R, Chang AJ, Rice M, Springer AL. Structural analysis of flagellar axonemes from inner arm dynein knockdown strains of *Trypanosoma brucei*. *Biochem J Soc Latinoam Microsc Electron Al.* 2012;36:133–41.
56. Jha BA, Gazestani VH, Yip CW, Salavati R. The DRBD13 RNA binding protein is involved in the insect-stage differentiation process of *Trypanosoma brucei*. *FEBS Lett.* 2015;589:1966–74.
57. Clayton CE. Life without transcriptional control? From fly to man and back again. *EMBO J.* 2002;21:1881–8.
58. Queiroz R, Benz C, Fellenberg K, Hoheisel JD, Clayton C. Transcriptome analysis of differentiating trypanosomes reveals the existence of multiple post-transcriptional regulons. *BMC Genomics.* 2009;10:495.
59. Haile S, Papadopoulos B. Developmental regulation of gene expression in trypanosomatid parasitic protozoa. *Curr Opin Microbiol.* 2007;10:569–77.
60. Gerber AP, Luschnig S, Krasnow MA, Brown PO, Herschlag D. Genome-wide identification of mRNAs associated with the translational regulator PUMILIO in *Drosophila melanogaster*. *Proc Natl Acad Sci USA.* 2006;103:4487–92.

61. Archer SK, Luu V-D, de Queiroz RA, Brems S, Clayton C. *Trypanosoma brucei* PUF9 regulates mRNAs for proteins involved in replicative processes over the cell cycle. *PLoS Pathog.* 2009;5:e1000565.
62. Archer SK, Inchaustegui D, Queiroz R, Clayton C. The cell cycle regulated transcriptome of *Trypanosoma brucei*. *PLoS ONE.* 2011;6:e18425.
63. Najafabadi HS, Lu Z, MacPherson C, Mehta V, Adoue V, Pastinen T, et al. Global identification of conserved post-transcriptional regulatory programs in trypanosomatids. *Nucleic Acids Res.* 2013;41:8591–600.
64. Mahmood R, Hines JC, Ray DS. Identification of *cis* and *trans* elements involved in the cell cycle regulation of multiple genes in *Crithidia fasciculata*. *Mol Cell Biol.* 1999;19:6174–82.
65. Avliyakov NK, Hines JC, Ray DS. Sequence elements in both the intergenic space and the 3' untranslated region of the *Crithidia fasciculata* KAP3 gene are required for cell cycle regulation of KAP3 mRNA. *Eukaryot Cell.* 2003;2:671–7.
66. Langousis G, Hill KL. Motility and more: the flagellum of *Trypanosoma brucei*. *Nat Rev Microbiol.* 2014;12:505–18.
67. Broadhead R, Dawe HR, Farr H, Griffiths S, Hart SR, Portman N, et al. Flagellar motility is required for the viability of the bloodstream trypanosome. *Nature.* 2006;440:224–7.
68. Ralston KS, Lerner AG, Diener DR, Hill KL. Flagellar motility contributes to cytokinesis in *Trypanosoma brucei* and is modulated by an evolutionarily conserved dynein regulatory system. *Eukaryot Cell.* 2006;5:696–711.

Publisher's Note

Springer Nature remains neutral with regard to jurisdictional claims in published maps and institutional affiliations.

Ready to submit your research? Choose BMC and benefit from:

- fast, convenient online submission
- thorough peer review by experienced researchers in your field
- rapid publication on acceptance
- support for research data, including large and complex data types
- gold Open Access which fosters wider collaboration and increased citations
- maximum visibility for your research: over 100M website views per year

At BMC, research is always in progress.

Learn more biomedcentral.com/submissions

